

PACS numbers: 32.80.Rm; 34.50.Fa
DOI: 10.1070/QE2006v036n08ABEH013180

Modulation and correlation of the radial and angular motions of a Rydberg electron in a resonance microwave field

P.A. Volkov, M.A. Efremov, M.V. Fedorov

***Abstract*. We discuss the physical sense and interpretation of the Maeda – Gallagher experiment (2004) in which the probability of ionisation of Rydberg Li atoms perturbed by the resonance microwave field by a short half-cycle pulse was measured. The periodic dependence of the ionisation probability w_i on the delay time t_0 of the half-cycle pulse with respect to the instant of switching on the microwave field is found. The oscillation period of the function $w_i(t_0)$ is equal to the Kepler period of a Rydberg electron. It is shown that the interpretation of this experiment by the authors in terms of localised wave packets has no grounds and neglects basic processes proceeding in the microwave field. An alternative interpretation is proposed and, as the first step, the structure of the Rydberg wave function formed in the resonance microwave field is studied.**

Keywords: *Rydberg electron, ionisation, wave functions.*

1. Introduction

The idea of formation of localised nonspreading quantum-mechanical wave packets has attracted the attention of researchers in fact with the advent of quantum mechanics, beginning from the works of Schrödinger [1]. Indeed, the states of the wave-packet type make it possible to find the similarity in the behaviour of quantum-mechanical and classical systems. However, as a rule, wave packets spread due to the wave nature of quantum mechanics. One of the exceptions is a harmonic oscillator in which localised quantum-mechanical states can be constructed which do not spread with time. Also, long-lived localised states maintained by an external electromagnetic field can be prepared. These are, for example, the so-called Troy Rydberg wave packets formed by a circularly polarised field and involved in the electron motion over a circular orbit [2]. The nonspreading Rydberg wave packets of a different type appear due to the Raman repopulation of levels in the interference stabilisation regime [3]. Finally, the narrow and nonspreading wave packets of the wave function of translational motion of atoms interacting with the field of a resonance standing light wave can be also produced in atomic optics [4]. According to the idea of Maeda and Gallagher [5], another method for formation of a narrow and nonspreading electron wave packet is the excitation of a Rydberg atom by a resonance microwave field. Unfortunately, in our opinion, this idea is not adequate to the experimental conditions [5], although the experiment itself is very interesting and its correct interpretation requires the independent theoretical study. Such an attempt is made in the present paper.

P.A. Volkov, M.A. Efremov, M.V. Fedorov A.M. Prokhorov General Physics Institute, Russian Academy of Sciences, ul. Vavilova 38, 119991 Moscow, Russia; e-mail: fedorov@ran.gpi.ru

Received 3 April 2006
Kvantovaya Elektronika **36** (8) 713 – 719 (2006)
Translated by M.N. Sapozhnikov

2. Experiment of Maeda and Gallagher

In experiment [5], the Li atoms were first excited to one of the Rydberg states by three successive 5-ns pulses from a dye laser according the scheme $2s \rightarrow 2p \rightarrow 3s \rightarrow 72p$. The spectral width of exciting pulses was small enough to provide the selective population of only the 72p level. Then, a linearly polarised resonance microwave field of strength $\varepsilon_0 = 1$ V cm^{-1} and angular frequency $\omega = 2\pi \times 17.258$ GHz was switched on. The microwave field frequency was resonant with the frequency $\omega \approx E_{73} - E_{72} \equiv \omega_K$ of the $n = 72 \rightarrow n = 73$ transition, where $E_n = -1/(2n^2)$ is the energy of the nth level of a hydrogen-like atom and $\omega_K = 1/n^3$ is the classical Kepler frequency. Hereafter, if the units of measurement are not indicated, the atomic system of units is assumed. The period $T_K = 2\pi/\omega_K$ corresponding to the Kepler frequency ω_K for $n = 72$ is 57 ps. Within the time t_0 after switching on the microwave field, the atoms were ionised by a subpicosecond half-cycle pulse. The dependence of the ionisation probability w_i on the instant t_0 of switching on the half-cycle pulse was measured. It was shown that this dependence was periodic, which is clearly demonstrated in Fig. 1 (Fig. 2 from [5]). The measured period of the function $w_i(t_0)$ proved to be equal to the oscillation period $2\pi/\omega$ of the microwave field, which in turn is approximately equal to the Kepler period T_K. Such a dependence of the function $w_i(t_0)$ was observed for more than 900 ns, which corresponds to more than 15 000 Kepler periods.

3. Authors' interpretation of the experiment of Maeda and Gallagher

The authors of paper [5] explain the results of their experiment by assuming that the microwave field acting on a Rydberg atom produces a long-lived nonspreading wave

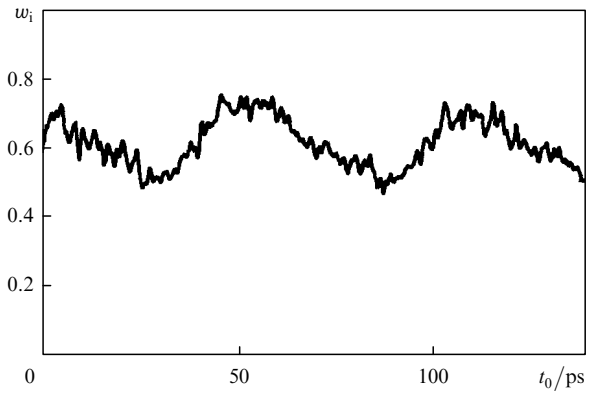

Figure 1. Periodic dependence of the ionisation probability w_i on the time interval t_0 between the instants of switching on the microwave field and half-cycle pulse. The data are taken from [5].

packet moving along the classical Kepler orbit strongly elongated along the polarisation direction of the microwave field.

The spatial distribution of the probability density (the square of the wave-function modulus) in such a state corresponds qualitatively to the picture shown in Fig. 2 (fragment of Fig. 1 from [5]). Within the framework of this model, the role of a half-cycle pulse is that it adds the momentum $\boldsymbol{p}_{\mathrm{HCP}} = \int \varepsilon_{\mathrm{HCP}}(t)\mathrm{d}t$ to the electron. If the directions of the microwave field and half-cycle pulse field coincide, the momentum $\boldsymbol{p}_{\mathrm{HCP}}$ is summed with the electron momentum on the Kepler orbit, resulting in the detachment of the electron from the ion, i.e. ionisation. If the electron momentum in the microwave field and the momentum $\boldsymbol{p}_{\mathrm{HCP}}$ are oppositely directed, they are mutually quenched, the electron movement slows down and no detachment of the electron from the ion (ionisation) occurs. This means that the ionisation probability depends on the microwave-field phase at which the half-cycle is switched on, which explains the observed oscillations of the ionisation probability depending on the instant of switching on the half-cycle pulse.

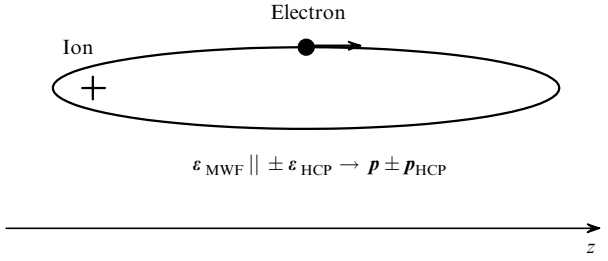

Figure 2. Probable picture of the motion of a localised electron wave packet along the Kepler orbit (fragment of Fig. 1 from [5]); $\varepsilon_{\mathrm{MWF}} = \varepsilon_0 \cos \omega t$ is the microwave field strength, p is the electron momentum at the Kepler orbit.

Let us emphasise that the described scheme concerns only the situation when the electron packet is strongly localised so that its dimensions are much smaller than the size of the Kepler orbit. It is well known [6–8] that such a localisation is possible only in the case of coherent population of many ($\Delta n \gg 1$) closely spaced Rydberg levels with different principal quantum numbers n (then, the packet width will be Δn times smaller than the Kepler orbit size). This requirement could not be fulfilled under experimental conditions [5]. For the microwave field strength of ~ 1 V cm^{-1}, only levels with $\Delta n = 1 - 2$ interact (are repopulated) efficiently, which agrees with the estimates made in paper itself [5]. Under such conditions, no localisation of the wave packet can occur, and the model of a localised nonspreading wave packet moving along the elongated Kepler orbit is invalid.

To support their interpretation, the authors [5] mention theoretical papers on the Floquet states of a one-dimensional Rydberg atom in a resonance field [9, 10]. They assert that one of the considered Floquet states corresponds to the model of a localised wave packet described above. They also affirm that the microwave field excites the incoherent superposition of approximately four most closely spaced Floquet states (see Fig. 4 in [5]). We believe that all this has little in common with the physics of processes proceeding in the Rydberg atom in the microwave field of such a low strength as in experiments [5].

Indeed, the Rydberg states of a hydrogen atom and hydrogen-like atoms are multiply degenerate (or almost degenerate) in the quantum numbers of the angular momentum l. The basic process proceeding in the Rydberg atom in a moderate resonance field is the population migration over l, i.e. over the degenerate sublevels of resonance levels (Fig. 3). This process cannot be taken into account within the framework of a one-dimensional model and, therefore, this model cannot describe the physics of effects observed in experiments [5]. Note also that the number of closely spaced Floquet states in the real situation of resonance at degenerate levels with $n = 72$ and 73 will be of the order of seventy rather than four. Because these levels are very closely spaced, they will be coherently (but not incoherently, as assumed in [5]) populated virtually at any method of switching on a resonance microwave field. It is clear that in this situation the description of the appearing state of the Rydberg electron in terms of the Floquet states will be very cumbersome, hardly realisable and unsuitable. Therefore, we do not use the theory of Floquet states in the formulation of the problem described below but find the direct solution of the initial problem. In other words, we find the solution of the nonstationary Schrödinger equation satisfying the correctly specified initial conditions and describing the evolution of the wave function of the Rydberg electron in the resonance microwave field.

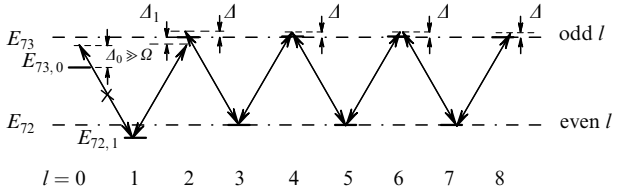

Figure 3. Diagram of the resonance levels degenerate or nearly degenerate in l, whose repopulation determines the population migration in the resonance microwave field. The positions of the $E_{73,0}$ and $E_{72,1}$ levels take into account the quantum-defect corrections (Ω, Δ and Δ_1 are the characteristic Rabi frequency and resonance detunings determined in section 4).

4. Formulation of the problem

Consider the nonstationary Schrödinger equation for a Rydberg electron in a resonance microwave field

$$i\frac{\partial \Psi(r,\theta,t)}{\partial t} = (H_0 - \boldsymbol{d}\,\varepsilon_0 \sin\omega t)\,\Psi(r,\theta,t), \tag{1}$$

where H_0 is the Hamiltonian of a free atom; $\boldsymbol{d}$ is the dipole moment of the atom; ε_0 is the microwave field strength amplitude; and r and θ are the modulus of the radius vector $\boldsymbol{r}$ of the Rydberg electron and angle between $\boldsymbol{r}$ and $\varepsilon_0 \| z$, respectively. We assume also that, as in experiment [5], the angular frequency of the microwave field $\omega = 2.664\times 10^{-6}$, which corresponds to the linear frequency $\nu = \omega/2\pi = 17.528$ GHz and the field variation period $T = 2\pi/\omega = 57$ ps. For the resonance levels with $n = 72$ and 73, the Kepler frequency is $\omega_K = 2.624 \times 10^{-6}$. Taking the quantum defect into account, the energies of Rydberg levels are $E_{n,l} = -1/[2(n-\delta_l)^2]$. The corrections δ_l for a lithium atom are well known [11]. They are not small only for the s and p states for which $\delta_0 = 0.4$, $\delta_1 = 0.047$. In fact the correction δ_0 provides so large a shift of the levels $E_{n,0}$ (compared to the hydrogen levels E_n) that transitions to the s levels and from them become nonresonant and are excluded in our calculations (see the energy level diagram taking the quantum defect into account and the scheme of quantum transitions in Fig. 3). The correction δ_1 is not so large but also not too small. The shift of the level $E_{72,1}$ determined by this correction is $\delta E_p = -1.26 \times 10^{-7}$ and should be taken into account in calculations. As for corrections δ_l with $l \geqslant 2$, they are so small that can be neglected, i.e. we can assume that $E_{n,l} = E_n \equiv -1/(2n^2)$ for all $l \geqslant 2$.

Due to the selection rules $\Delta l = \pm 1$ for dipole transitions and the initial population of the level with $l = 1$ ($n = 72$), only the $E_{72,l}$ levels with odd l and the $E_{73,l'}$ levels with even l' are populated during interaction with the microwave field. For transitions between these levels $(72, l \rightleftarrows 73, l \pm 1)$, the resonance detuning is

$$\Delta_l = \omega + E_{72,l} - E_{73}$$

$$= \begin{cases} \omega - \omega_K \equiv \Delta = 4.1 \times 10^{-8}, & l \geqslant 2, \\ \omega - \omega_K - \delta E_p = \Delta - \delta E_p \equiv \Delta_1 = -8.5 \times 10^{-8}, & l = 1. \end{cases} \tag{2}$$

The difference between Δ and Δ_1 is clearly seen in Fig. 3. We will consider transitions between Rydberg levels with $n < 72$ and $n > 73$ as nonresonant ones because the corresponding detunings are smaller than the Rabi frequency (estimates are presented below).

We solve the Schrödinger equation (1) by expanding the wave function Ψ in a series of free-atom Hamiltonian eigenfunctions:

$$\psi_{n,l,m_l=0}(\boldsymbol{r}) \equiv \psi_{n,l} = \left(\frac{2l+1}{2}\right)^{1/2} P_l(\cos\theta) R_{n,l}(r), \tag{3}$$

where $P_l(\cos\theta)$ are Legendre polynomials; $R_{n,l}(r)$ is the radial part of the wave function $\psi_{n,l}$. According to the approximations made above, we take into account only resonance terms in the expansion of Ψ in $\psi_{n,l}$, i.e. the terms with $n = 72$ and 73:

$$\Psi(r,\theta,t) = \sum_{\text{odd } l \geqslant 1} \exp(-iE_{72,l}t)\, C_l(t)\psi_{72,l}(r,\theta)$$

$$+ \exp(-iE_{73}t) \sum_{\text{even } l \geqslant 2} D_l(t)\psi_{73,l}(r,\theta), \tag{4}$$

where C_l and D_l are the probability amplitudes of finding an atom in the states $|72, l\rangle$ and $|73, l\rangle$, respectively.

The matrix elements of dipole transitions between the states $|72, l\rangle$ and $|73, l'\rangle$ can be approximated by quasiclassical expressions found in [12]. It is convenient to introduce the reduced matrix elements of the dipole moment by expressions

$$V_l^- = \frac{\langle n+1, l-1|d_z|n,l\rangle}{n(n+1)}$$

$$= \frac{l}{(4l^2-1)^{1/2}}[J_1'(\epsilon_l) - J_1(\epsilon_l)(\epsilon_l^{-2}-1)^{1/2}], \tag{5}$$

$$V_l^+ = \frac{\langle n+1, l|d_z|n,l-1\rangle}{n(n+1)}$$

$$= \frac{l}{(4l^2-1)^{1/2}}[J_1'(\epsilon_{l-1}) + J_1(\epsilon_{l-1})(\epsilon_{l-1}^{-2}-1)^{1/2}], \tag{6}$$

where $J_1(x)$ is the first-order Bessel function; $J_1'(x) \equiv dJ_1(x)/dx$ is its derivative; $\epsilon_l = \{1 - (l+\frac{1}{2})^2/[n(n+1)]\}^{1/2}$; $l \geqslant 1$; and $n = 72$ in the case under study.

The dependence of matrix elements $V_l^{\pm}(l)$ on l is shown in Fig. 4. One can easily see that $V_l^+ \geqslant V_l^-$ for all $l \geqslant 1$, i.e. the Bethe rule is fulfilled for Coulomb dipole matrix elements: as the principal quantum number n changes, the orbital momentum l changes most likely in the same direction as n. One can see from Fig. 4 that the values of $V_l^{\pm}$ for small l are approximately equal to 0.2, which corresponds to the characteristic Rabi frequency $\Omega \approx 0.1n(n+1)\varepsilon_0 \sim 10^{-7}$. This value is larger than the resonance detuning (2) for all the states under study, i.e. $\Omega > |\Delta_l|$. Therefore, all the sublevels $E_{n,l}$ of the Rydberg levels with $n = 72$ and 73 are strongly coupled with each other. On the other hand, the resonance detuning for the $n \rightleftarrows n+1$ transition with $n \neq 72$ can be estimated as $\Delta^{(n)} \sim -3(n-72)/n^4 \sim (n-72) \times 10^{-7} > \Omega$. This inequality justifies our assumption that transitions to the levels with $n > 73$ and $n < 72$ can be approximately neglected. Never-

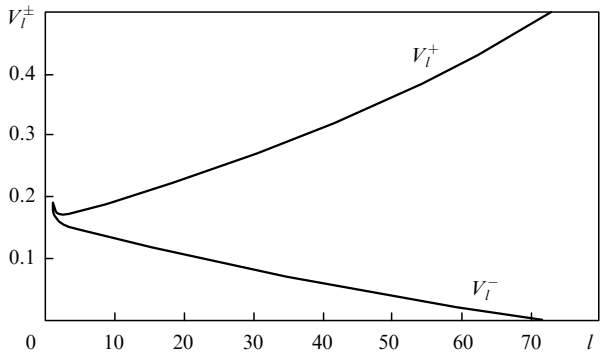

Figure 4. Dipole matrix elements V_l^- (5) and V_l^+ as functions of l.

theless, the levels located close to the resonance levels (with $n = 74$ and 71) can be populated to some degree even in the field of strength $\sim 1\ \mathrm{V\ cm^{-1}}$. These processes will be considered separately. However, we believe that such an extension of the basis for the expansion of the wave function Ψ will not change qualitatively the results and conclusions obtained in this paper.

Finally, note that the decrease in the matrix element V_l^- with increasing l (Fig. 4) restricts the growth of the angular momentum during population migration in the direction of greater values of l.

By using the rotating wave approximation, we reduce the Schrödinger equation (1) for the wave function $\Psi(r, \theta, t)$ (4) to the system of ordinary differential equations

$$\begin{aligned} \mathrm{i}\frac{\mathrm{d}C_l}{\mathrm{d}t} &= \frac{1}{2}n(n+1)\varepsilon_0[\exp(\mathrm{i}t\Delta)\, V_l^- D_{l-1} \\ &\quad + \exp(\mathrm{i}t\Delta_l) V_{l+1}^+ D_{l+1}],\ l \geqslant 1, \\ \mathrm{i}\frac{\mathrm{d}D_l}{\mathrm{d}t} &= \frac{1}{2}n(n+1)\varepsilon_0[\exp(-\mathrm{i}t\Delta_{l-1})\, V_l^+ C_{l-1} \\ &\quad + \exp(-\mathrm{i}t\Delta) V_{l+1}^- C_{l+1}],\ l \geqslant 2 \end{aligned} \tag{7}$$

with the initial conditions

$$C_l(t=0) = \delta_{l,1}, \quad D_l(t=0) = 0. \tag{8}$$

To exclude the nonresonance $72\mathrm{p} \rightarrow 73\mathrm{s}$ transition (deleted in Fig. 3), we should set $V_1^- = 0$ in the first of the equations in (7).

By solving numerically the system of equations (7), we find the functions $C_l(t)$ and $D_l(t)$ determining all the parameters of the Rydberg state of an electron in the resonance microwave field. In particular, the expression for the time-dependent probability density ρ of finding the electron in the vicinity of point (r, θ) has the form

$$\begin{aligned} \rho(r,\theta,t) &= \frac{\mathrm{d}w}{\mathrm{d}r\,\mathrm{d}\theta} = r^2 \sin\theta |\Psi(r,\theta,t)|^2 \\ &= r^2 \sin\theta \Bigg\{ \Bigg| \sum_{\text{even } l} D_l(t)\, P_l(\cos\theta)\, R_{n+1,l}(r) \Bigg|^2 \\ &\quad + \Bigg| \exp(-\mathrm{i}\delta E_\mathrm{p} t) C_1(t)\, P_1(\cos\theta)\, R_{n,1}(r) \\ &\quad + \sum_{\text{odd } l>1} C_l(t)\, P_l(\cos\theta)\, R_{n,l}(r) \Bigg|^2 \\ &\quad + \Bigg[\exp(\mathrm{i}\omega t) \sum_{\substack{\text{odd } l \\ \text{even } l'}} \exp(-\mathrm{i}t\Delta_l) C_l(t) D_{l'}^*(t) \\ &\quad \times P_l(\cos\theta) P_{l'}(\cos\theta) R_{n,l}(r) R_{n+1,l'}(r) + \text{c.c.} \Bigg] \Bigg\}. \end{aligned} \tag{9}$$

This function and a number of quantities determining the evolution of the state of the Rydberg electron in the resonance microwave field are analysed in detail in the next section. Here we point out only that, first, under considered conditions the oscillations at the field frequency approximately equal to the Kepler frequency ($\omega \approx \omega_\mathrm{K}$) are fastest, in particular, compared to the characteristic times of variations in functions $C_l(t)$ and $D_l(t)$. Therefore, rapid oscillations of the probability density (9) at frequency $\omega \approx \omega_\mathrm{K}$ appear only in the interference term (in brackets). If this term does not make a contribution to the mean values of some operators, these values do not exhibit oscillations with the field period. Such examples are presented below. Second, below we will not differentiate oscillations at the field frequency from those at the Kepler frequency. The more so as follows from a detailed analysis, the frequency of these rapid oscillations is not rigorously defined and is subject to small and slow variations. We will not analyse this here in detail.

5. Results of calculations

5.1 Population of the $E_{n,l}$ sublevels of resonance states

Figure 5 shows the time dependence of the mean value of the quantum number of the angular momentum

$$\bar{l}(t) = \sum_{\text{odd } l} l\, |C_l(t)|^2 + \sum_{\text{even } l} l\, |D_l(t)|^2. \tag{10}$$

This figure demonstrates three evolution stages of the electrons state: the initial transient period when $\bar{l}(t)$ increases more or less monotonically, the period of some decrease in $\bar{l}(t)$, and the long period of more or less stationary behaviour of the function $\bar{l}(t)$. The oscillations of the function $\bar{l}(t)$ at the second and third stages are similar to Rabi oscillations. However, because we consider a multilevel system, the oscillations are more complicated than simple sinusoidal oscillations of the population in a two-level system. The function $\bar{l}(t)$ does not experience oscillations at the Kepler frequency, which is clearly seen already from its definition (10).

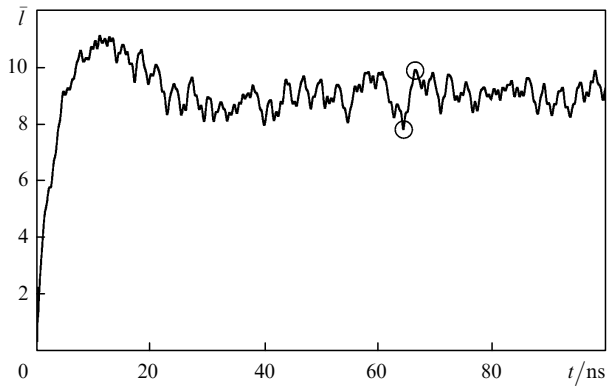

Figure 5. Time evolution of the mean quantum number of the angular momentum $\bar{l}(t)$. The circles indicate the instants of time for which the curves in Fig. 6 are plotted.

Although the time dependence of the mean angular momentum is quite informative, it does not describe all the features of population migration over the $E_{72,l}$ and $E_{73,l}$ levels. Such data can be obtained from a direct analysis of the probability distribution of population of the sublevels with different values of l. The probabilities $w(l)$ are defined as $|C_l|^2$ for odd l and $|D_l|^2$ for even l. Two examples of such distributions are presented in Fig. 6. The curves correspond

to the instants $t = 64.451$ and 66.559 ns. These instants are indicated by circles in Fig. 5. They correspond to the local minimum at $t = 64.451$ ns and maximum at $t = 66.559$ ns of the function $\bar{l}(t)$. Note, first, that the distributions $w(l)$ are rather broad and, second, they contain small values of the angular momentum with a rather large weight. Like $\bar{l}(t)$, the probabilities $w(l, t)$ do not oscillate at the Kepler frequency but exhibit quasi-Rabi oscillations.

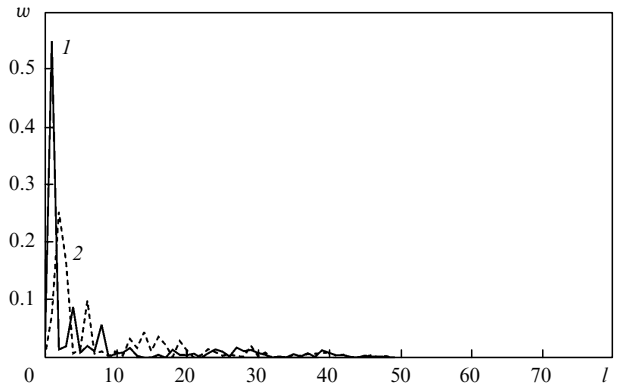

Figure 6. Probability distributions $w(l)$ for the population of the $E_{72,l}$ and $E_{73,l}$ levels at $t = 64.451$ (*1*) and 66.559 ns (*2*).

$[R_{72,1}(r)]$ and angular $[P_1(\cos\theta)]$ wave functions, and there is no correlation between them. The radial and angular variables are mixed in the microwave field, the total wave function $\Psi(r, \theta, t)$ (4) is not factorised, and the correlation coefficient increases on the average up to ~ 3.5, which points to a rather high correlation or coupling of the radial and angular motions in a Rydberg atom in a resonance microwave field.

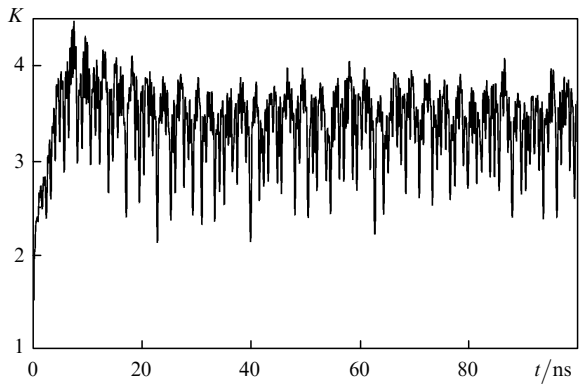

Figure 7. Time dependence of the Schmidt parameter K characterising the correlation degree of the electron radial and angular motions.

5.2 Correlation of the radial and angular motions

Another parameter of interest, which was calculated, is the Schmidt parameter K [13] characterising the degree of correlation of the electron radial and rotation motion. In two-particle systems, this parameter is used to characterise the entanglement degree of particle variables in the wave function or the entanglement degree of quantum states [14]. In the case of one particle with two degrees of freedom, it seems more reasonable to speak about the degree of correlation of motions along these two degrees of freedom. However, irrespective of the terminology, in any case the Schmidt parameter indicates to what degree the wave function of two variables differs from the factorised wave function given by the product of two functions, each of them being dependent on only one of the two variables. In the case of the factorised wave function, both correlations and entanglement are absent, and the Schmidt parameter is unity. The larger is this parameter, the higher is the correlation (entanglement) degree. In the case of systems with two continuous variables, the Schmidt parameter is conveniently defined as [15]

$$K = \left\{ \int r^2 \mathrm{d}r \sin\theta \, \mathrm{d}\theta r'^2 \mathrm{d}r' \sin\theta' \mathrm{d}\theta' \right.$$

$$\left. \times \Psi(r, \theta) \, \Psi^*(r', \theta) \Psi^*(r, \theta') \Psi(r', \theta') \right\}^{-1}. \qquad (11)$$

The calculated time dependence of the parameter K is presented in Fig. 7. As a whole, the dependence $K(t)$ is similar to the dependence $\bar{l}(t)$ (Fig. 5), although quasi-Rabi oscillations of the correlation coefficient are more pronounced than oscillations of the mean quantum number of the angular momentum. At the initial instant, $K(0) = 1$ because the initial wave function is the product of the radial

5.3 Radial distribution of the probability density

Figure 8 shows the dependence of the probability density $\rho(r, \theta, t)$ (9) on the radius r for a fixed angle θ ($\theta = 0.7$ rad) at instants $t = 22.935$ and 22.962 ns differing by half the Kepler period. One can see that the probability density distribution over the radius r in the specified direction θ noticeably changes after half the field period. By repeating calculations in the interval of the order of several field periods, we can easily see that the time dependence of the probability density $\rho(r, \theta, t)$ at fixed θ contains both a slowly varying component and a component oscillating with the Kepler period. It is interesting to note, however, that the radial probability density integrated over all directions

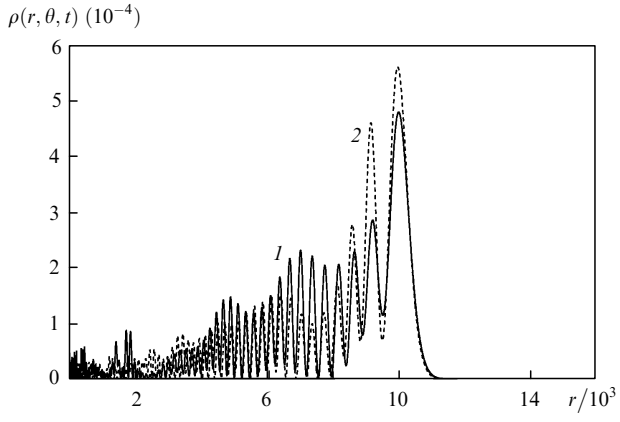

Figure 8. Probability density $\rho(r, \theta, t)$ (9) for $\theta = 0.7$ rad, $t = 22.935$ (*1*) and 22.962 ns (*2*).

$$\rho(r;\, t) = \int_0^{\pi} \mathrm{d}\theta\, \rho(r, \theta, t) \tag{12}$$

has no oscillations with the Kepler period. This conclusion follows directly from the general expression for the probability density $\rho(r, \theta, t)$ (9). Due to the orthogonality of Legendre polynomials P_l and $P_{l'}$ with different l and l', the interference term in the expression for $\rho(r, \theta, t)$ [term in the brackets in (9)] vanishes upon integration over θ. This means that the mean values of any operators independent of θ also do not contain components oscillating at the Kepler frequency. In particular, this also concerns the time-dependent the mean radius $\bar{r}(t)$ of the wave function of an electron. Figure 9a shows the fragment of the time dependence of this function. One can see that the function $\bar{r}(t)$ is monotonic and has no oscillations in the interval of the order of five Kepler periods.

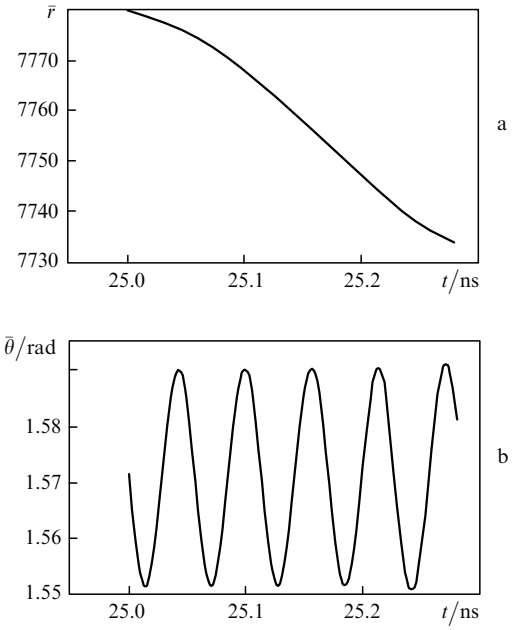

Figure 9. Time dependences of the mean distance from an electron to the ion core $\bar{r}(t) = \langle \Psi(t)|r|\Psi(t)\rangle$ (a) and of the mean angle $\bar{\theta}(t) = \langle \Psi(t)|\theta|\Psi(t)\rangle$ (b).

Although the absence of oscillations of the mean values of operators independent of θ with the Kepler period is formally explained by the orthogonality of Legendre polynomials, it is nevertheless interesting to elucidate in detail how oscillations with the Kepler period disappear during angular averaging. This mechanism is illustrated to some degree by the dependence on θ of the radius r averaged only over r itself but not over the angle θ (Fig. 10):

$$\bar{r}(\theta,\, t) = \int_0^{\infty} r^3 \mathrm{d}r\, |\Psi(r, \theta, t)|^2. \tag{13}$$

The three curves in Fig. 10 correspond to three different evolution stages of the system: before microwave field switching on ($t = 0$), the stage corresponding to the increase in $\bar{l}(t)$ in Fig. 5 ($t = 10$ ps), and the quasi-stationary regime stage ($t = 15$ ns). The disappearance of oscillations upon the averaging of $\bar{r}(\theta, t)$ over θ is simply explained in the

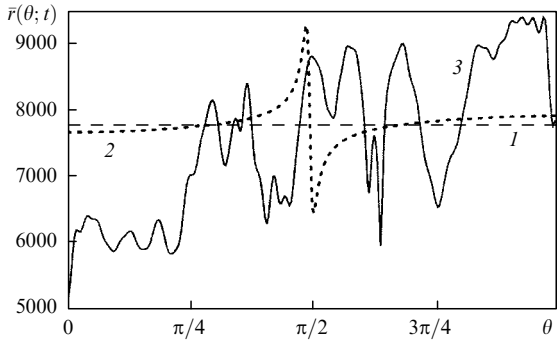

Figure 10. Mean radius of the electron – ion distance as a function of the angle θ for $t = 0$ (*1*), 10 ps (*2*), and 15 ns (*3*).

intermediate regime. The excess of the area under curve (*2*) in the region of maximum (to the left of the point $\theta = \pi/2$) is compensated for to a great extent by the defficiency in the area under the curve in the region of minimum (to the right of the point $\theta = \pi/2$), and the sum of these contributions to the integral over θ proves to be approximately the same as for $t = 0$. After half the Kepler period, the maximum and minimum of curve (*2*) are interchanged and the integral effect remains almost unchanged, i.e. oscillations are absent. Thus, in this case the disappearance of oscillations with the Kepler period upon averaging over θ is directly related to the structure of the curve $\bar{r}(\theta; t)$. The oscillations of the mean radius $\bar{r}(\theta; t)$ are most pronounced in the vicinity of the point $\theta = \pi/2$. The oscillations of $\bar{r}(\theta; t)$ to the left and right of the point $\theta = \pi/2$ are out of phase and are mutually compensated for upon integration over θ.

Unfortunately, the function $\bar{r}(\theta; t)$ in the quasi-stationary regime is strongly complicated and its behaviour cannot be explained so clearly as above. In this case, only a formal explanation by the orthogonality of Legendre polynomials remains.

5.4 Angular distribution of the probability density

One can see from Fig. 9b that the behaviour of the mean angle $\bar{\theta}(t)$ considerably differs from that of the mean radius $\bar{r}(t)$: the function $\bar{\theta}(t)$ oscillates with the Kepler frequency, whereas $\bar{r}(t)$ changes monotonically (for the time of the order of a few Kepler periods). This is explained by the fact that, unlike Legendre polynomials, the radial wave functions $R_{n,l}$ and $R_{n',l'}$ are not mutually orthogonal at different l and l'. For this reason, the interference term in expression (9) for the probability density $\rho(r, \theta, t)$ does not vanish upon integration over r.

Finally, we present the data on the angular distribution of the probability density. The angular probability density

$$\rho(\theta; t) = \int_0^{\infty} \mathrm{d}r\, \rho(r, \theta, t) \tag{14}$$

in Fig. 11 is presented in polar coordinates. This means that the angle θ is measured from the positive direction of the z axis both clockwise and counter-clockwise. The distance from the coordinate origin to points in the curves is $\rho(\theta; t)$. The two curves correspond to two instants of time separated by half the Kepler period.

One can see from Fig. 11 that the angular distribution of the probability density of finding an electron in the vicinity

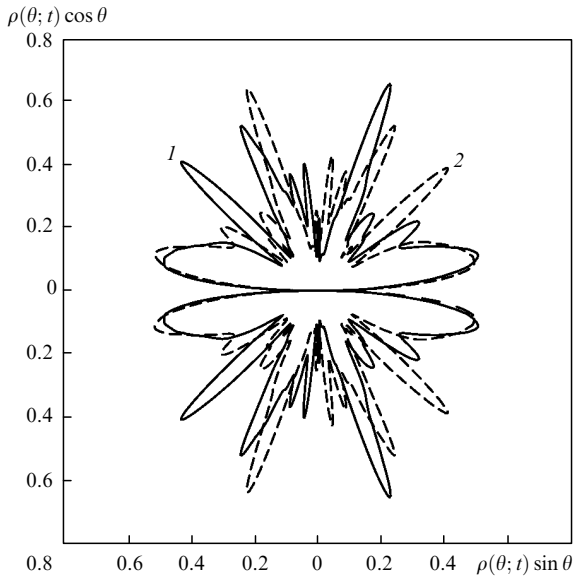

Figure 11. Angular probability densities $\rho(\theta;t)$ for $t = 22.935$ (*1*) and 22.962 ns (*2*).

of directions determined by the angle θ is quite irregular. In principle, we can say about the formation of a series of angle-localised wave packets in the microwave field. One can clearly see changes in the distribution upon the time shift by half the field period. These changes repeat through the period, i.e. the angular distribution of the probability density oscillates with the Kepler period.

6. Conclusions

In summary, we repeat that the interaction of a Rydberg atom with a resonance microwave field under experimental conditions [5] is not accompanied by the formation of an electron wave packet localised along the radial variable and moving along the Kepler orbit as a classical particle. The absence of such a localisation is explained by the fact that many Rydberg levels with different values of the principal quantum number n are not populated in a relatively weak resonance microwave field. On the other hand, the resonance field can produce the efficient repopulation of the sublevels of the resonance states with different quantum numbers l of the angular moment. We believe that it is this process that plays a key role in the interaction of a Rydberg atom with a relatively weak but resonance field. The problem of description of the repopulation of the sublevels of the resonance states with different quantum numbers l of the angular momentum excludes in principle the use of any one-dimensional atomic models.

Although the resonance microwave field of a moderate intensity does not provide the radial localisation of the wave function, it causes the modulation (at the field frequency) of both the radial and angular motions of the electron. Undoubtedly, this modulation is responsible for the periodic dependence of the ionisation probability of the atom on the time of switching on the ionising half-cycle pulse. We hope to return in the future to the description of the ionisation process and to obtain the explicit dependences of the ionisation probability on the parameters of the half-cycle pulse and microwave field.

In this paper, we have studied in detail the radial and angular distributions of the probability density and have shown that the radial and angular motions are strongly mutually correlated. One of the differences between the modulations of the angular and radial motions of the electron in the resonance microwave field is that the radial distribution of the probability density integrated over angles does not oscillate with the Kepler frequency, whereas such oscillations are observed in the angular distribution integrated over the radius.

The angular structure of the wave function of the electron in the microwave field proves to be rather complicated and irregular, containing a series of comparatively narrow peaks. In principle, such a structure can be interpreted as a series of relatively narrow angular wave packets localised over the angle θ and maintained by the microwave field. However, they are not localised in the radial direction and cannot be associated with a classical particle moving along the Kepler orbit.

Acknowledgements. This work was partially supported by the Russian Foundation for Basic Research (Grant No. 05-02-16469) and Grant No. MK 1283.2005.2 of the President of the Russian Federation.

References

1. Schrödinger E. *Naturwissenschaften*, **14**, 664 (1926).
2. Bialynicki-Birula I., Kalinski M., Eberly J.H. *Phys. Rev. Lett.*, **73**, 1777 (1994); Kalinski M. et al. *Phys. Rev. A*, **67**, 032503 (2003).
3. Fedorov M.V., Fedorov S.M. *Opt. Express*, **3**, 271 (1998).
4. Chudesnikov D.O., Yakovlev V.P. *Laser Phys.*, **1**, 110 (1991); Oberthaler M.K. et al. *Phys. Rev. Lett.*, **77**, 4980 (1996); Berry M.V., O'Dell D.H.J. *J. Phys. A*, **31**, 2093 (1998); Stutzle R. et al. *Phys. Rev. Lett.*, **95**, 110405 (2005).
5. Maeda H., Gallagher T.F. *Phys. Rev. Lett.*, **92**, 133004 (2004).
6. Fedorov M.V. *Atomic and Free Electrons in a Strong Light Field* (Singapore: World Scientific, 1997).
7. Ten Wolde A., Noordam L.D., Lagendijk A., van Linden van den Heuvell H.B. *Phys. Rev. Lett.*, **61**, 2099 (1988).
8. Yeasell J.A. *Phys. Rev. A*, **40**, 5040 (1989).
9. Buchleitner A., Delande D. *Phys. Rev. Lett.*, **75**, 1487 (1995).
10. Jensen R.V., Susskind S.M., Sanders M.M. *Phys. Rep.*, **201**, 1 (1991).
11. Radzic A.A., Smirnov B.M., in *Dissociation Energies (Reference on Atoms and Ions)* (Berlin: Springer-Verlag, 1985, Springer Series in Chemical Physics) Vol. 31.
12. Bureeva L.A. *Astronom. Zh.*, **45**, 1215 (1968).
13. Grobe R., Rzazewski K., Eberly J.H. *J. Phys. B*, **27**, L503 (1994).
14. Fedorov M.V., Efremov M.A., Kazakov A.E., Chan K.W., Law C.K., Eberly J.H. *Phys. Rev. A*, **69**, 052117; **72**, 032110 (2005).
15. Fedorov M.V., Efremov M.A., Volkov P.A., Eberly J.H. *J. Phys. B* (2006) (in press).